

QCI Qbsolv Delivers Strong Classical Performance for Quantum-Ready Formulation

Michael Booth
Quantum Computing Inc.
Leesburg, VA, USA

Jesse Berwald
Quantum Computing Inc.
Leesburg, VA, USA
ORCID 0000-0003-4741-2427

Uchenna Chukwu
Quantum Computing Inc.
Leesburg, VA, USA
ORCID 0000-0002-1311-3827

John Dawson
Quantum Computing Inc.
Leesburg, VA, USA

Raouf Dridi
Quantum Computing Inc.
Leesburg, VA, USA

DeYung Le
Quantum Computing Inc.
Leesburg, VA, USA

Mark Wainger
Quantum Computing Inc.
Leesburg, VA, USA

Steven P. Reinhardt
Quantum Computing Inc.
Leesburg, VA, USA
ORCID 0000-0003-4355-6693

Abstract—Many organizations that vitally depend on computation for their competitive advantage are keen to exploit the expected performance of quantum computers (QCs) as soon as *quantum advantage* is achieved. The best approach to deliver hardware quantum advantage for high-value problems is not yet clear. This work advocates establishing *quantum-ready* applications and underlying tools and formulations, so that software development can proceed now to ensure being ready for quantum advantage. This work can be done independently of which hardware approach delivers quantum advantage first. The quadratic unconstrained binary optimization (QUBO) problem is one such quantum-ready formulation. We developed the next generation of qbsolv, a tool that is widely used for sampling QUBOs on early QCs, focusing on its performance executing purely classically, and deliver it as a cloud service today. We find that it delivers highly competitive results in all of quality (low energy value), speed (time to solution), and diversity (variety of solutions). We believe these results give quantum-forward users a reason to switch to quantum-ready formulations today, reaping immediate benefits in performance and diversity of solution from the quantum-ready formulation, preparing themselves for quantum advantage, and accelerating the development of the quantum computing ecosystem.

Index Terms—quantum computing, hybrid quantum-classical computing, constrained discrete optimization, quadratic unconstrained binary optimization (QUBO), quantum algorithms, quantum advantage, QAOA

I. INTRODUCTION

Quantum computers have the potential to enable stunning advances, improving the human condition in profound ways – e.g., saving lives via faster and more effective drug designs and reducing humanity’s impact on the Earth’s environment via better processes for manufacturing fertilizer. Today, however, no quantum computer has yet delivered *quantum advantage*, i.e., better performance on a real-world problem, and predictions of when quantum advantage will be achieved range from 1 to 15 years in the future. This uncertainty presents a real challenge to quantum-forward organizations wishing to exploit the power of QCs as soon as possible.

We are implementing an approach that recognizes the vital role that software will play in delivering the performance potential of QCs. This approach consists of four main threads. First, given the uncertainty in when quantum advantage will be delivered and in the details of potential early QCs (e.g., architecture, number of qubits, and gates natively implemented) that may deliver quantum advantage, application-development formulations and tools must insulate developers from that uncertainty, including machine-specific details, to the extent practical while still delivering quantum advantage to user applications as soon as QC hardware makes it possible [1]. (Obviously the presence or absence of huge QC performance speed-ups cannot be hidden, but the differences in programming those QCs can be.) Second, tools should foster the development of hybrid quantum-classical methods that use early (small, less-than-robust) quantum processors to deliver the best practical performance. Third, tools must deliver superior performance now; obviously this will not be the thousand-fold or million-fold speed-ups that people expect from QCs, but convincing quantum-forward organizations to adopt quantum-ready applications and tools requires immediate benefit be delivered. Lastly, achieving these goals in a fully general way appears daunting in the extreme, so narrowing the focus to a particular type of quantum-ready problem type is probably necessary to achieve near-term success.

One quantum-ready formulation is the quadratic unconstrained binary optimization (QUBO) problem, also known as the transverse-field Ising model to physicists, the binary quadratic problem to operations researchers, and the probabilistic graphical model to statisticians. The QUBO has much to recommend it. It solves a wide variety of discrete combinatorial optimization problems effectively [2], maps directly to annealing-based QCs [3] and effectively to gate-model QCs, and has a rich and expanding reservoir of research behind it [4], [5]. QUBO formulations have been used for QC-targeted applications for graph partitioning for molecular dynamics simulations [6], for protein design [7],

for reducing traffic flow [8], and for optimizing workflows within factories [9]. While it has many strengths, the QUBO requires careful use, as the tuning of Lagrange multipliers, balancing numerical values so that feasible solutions have better energies than non-feasible solutions, complicates getting good results. Methods have been proven for executing QUBOs, on annealing-based QCs [10], [11], even QUBOs bigger than the quantum processor, and on gate-model QCs via the Quantum Approximate Optimization Algorithm (QAOA) [12], so the quantum-readiness of the QUBO formulation is established. In sum, there is considerable evidence the QUBO formulation can play an effective role in solving discrete combinatorial optimization problems in a quantum-ready way.

TABLE I: Selected MQlib Instances

Instance name	Number of variables	Number of nonzeros	Density
g000283	3,364	406,237	0.0718
g000377	3,398	3,966	0.0007
g000421	2,034	7,756	0.0038
g000432	2,153	250,371	0.1081
g000476	8,000	64,177	0.0020
g000495	5,438	3,151,321	0.2132
g000503	5,046	5,695,279	0.4474
g000524	2,218	336,856	0.1370
g000644	10,000	79,778	0.0016
g000788	2,342	2,404,777	0.8772
g000802	3,956	1,034,494	0.1322
g000969	2,453	2,581,494	0.8584
g000989	2,319	2,318	0.0009
g001086	3,706	10,898	0.0016
g001269	2,294	4,588	0.0017
g001327	2,318	796,617	0.2966
g001337	2,850	208,125	0.0513
g001345	5,066	9,530,811	0.7429
g001393	3,938	6,412,304	0.8272
g001469	2,412	1,345,896	0.4629
g001581	2,383	2,447,660	0.8624
g001651	5,819	16,452,342	0.9719
g001883	6,831	13,662	0.0006
g001913	3,865	5,635,669	0.7547
g002034	2,528	1,119,904	0.3506
g002204	5,368	6,318,136	0.4386
g002207	2,677	2,665,638	0.7442
g002300	5,038	11,889,413	0.9370
g002312	6,395	3,830,605	0.1874
g002332	3,181	1,117,657	0.2210
g002370	3,884	6,327,201	0.8391
g002440	2,242	110,979	0.0442
g002512	4,731	1,386,782	0.1239
g002527	5,378	8,507,996	0.5884
g002563	6,279	3,705,823	0.1880
g002569	2,815	4,162	0.0011
g002586	2,079	345,114	0.1598
g002600	2,432	2,503,793	0.8470
g002898	2,041	1,795,003	0.8622
g003059	3,447	813,960	0.1370
g003198	3,972	5,850,724	0.7419
g003215	2,206	2,272	0.0009
imgseg_216041	7,724	11,689	0.0004
imgseg_376020	7,455	13,682	0.0005
p7000_2	7,001	19,505,601	0.7960

Our approach respects another important constraint – commercial viability. We are implementing QCI’s Mukai

middleware with a broad user base and a software architecture in mind, knowing that today’s version will morph in light of tomorrow’s better understanding of both quantum hardware and software. We have a persistent focus on performance, notably the sampling core of QCI qbsolv but also efficient interfaces in terms of execution time and memory consumption. And, we deliver a discrete constrained-optimization sampler in the cloud, running purely classically today and quantum-ready for the future, and delivering superior performance today. The approach is also cost effective; the test runs in this paper were run on virtual machines in the cloud with a list price less than five dollars per hour. This makes it practical for quantum-forward users to shift development and execution of applications requiring the speed of future QCs to a quantum-ready software base today.

II. IMPLEMENTATION AND EXPERIMENTAL DESIGN

A. MQlib and Selected Instances

MQlib [13] is a collection of 3298 QUBOs (or maximum cut problems readily converted to QUBOs) and 37 QUBO-sampling heuristics open-sourced in 2015. In addition to that aspect of their work, Dunning et al. studied the execution behavior of each instance on the heuristics to derive suggested runtimes that distinguished well-performing heuristics from poorly performing ones. D-Wave personnel [14] selected 45 *hard* MQlib instances, defined as having the maximum suggested runtime of 1200 seconds and only one heuristic achieving the best reported solution, leaving aside any instances with more than 10,000 variables. We used the same set of 45 instances, listed in Table I, to make our results more easily comparable and to build consensus for a community-supported benchmark.

B. QCI Qbsolv Implementation

The MQlib QUBOs were solved with QCI qbsolv, a component of the quantum-ready QCI Mukai software stack. Derived from the open-source qbsolv [11], QCI qbsolv has been reimplemented to deliver exceptional performance (quality, speed, and diversity of results) from highly parallel classical processors, exploiting advanced tabu search techniques. For these runs, we requested QCI qbsolv to favor quality of results (lowest energy) over fastest runtime, and return the best 700 answers obtained. We ran each problem 5 times and use the results of the run gaining the best energy value for evaluation.

C. Computer Specs

For these runs, we executed QCI qbsolv in its current typical setting, an AWS instance visible via a Python API exercising a REST API. The AWS instance was a c5.24xlarge Linux instance, including 96 Intel Xeon cores running at 3.0 GHz (up to 3.4GHz via Turbo Boost) and 192 GiB of RAM. QCI qbsolv was given a time limit of 1200 seconds for all problems, equaling the time limit used in the MQlib runs. These results were obtained on Mukai 1.1.

D. Performance Metrics

Measuring the performance of a quantum computer is quite different from measuring the performance of a classical computer, in that the QC exploits probabilistic quantum effects and hence the QC's results are, in general, nondeterministic [15]. The QUBO form represents NP-hard optimization problems, real-world instances of which will be prohibitively expensive to solve exactly, and hence the quality of the solution will typically vary from run to run due to the probabilistic nature of the QC. Quality of solution, often stated for the QUBO as best or lowest energy, is one dimension of QC performance that will be important, and it is the dimension that is the first focus of this work. The second dimension we focus on is the execution time required to obtain those low-energy solutions. Third is the diversity of the best or *elite* solutions, often measured pair-wise by the Hamming distance. The relative importance of these 3 dimensions is application dependent. In a case where the selected solution will be realized a great many times, such as financial optimization, even a slightly better solution may be high value. In another case, such as changing a logistics schedule to respond to a dynamic situation, fixed time to respond to an external stimulus may mean that execution time below some limit may be critical. In yet another case, for example protein design, delivering many possible solutions to be compared against other criteria may be most important.

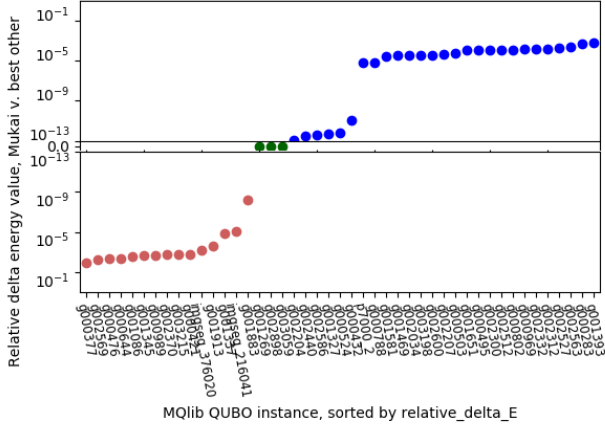
III. RESULTS AND DISCUSSION

A. Best Energy

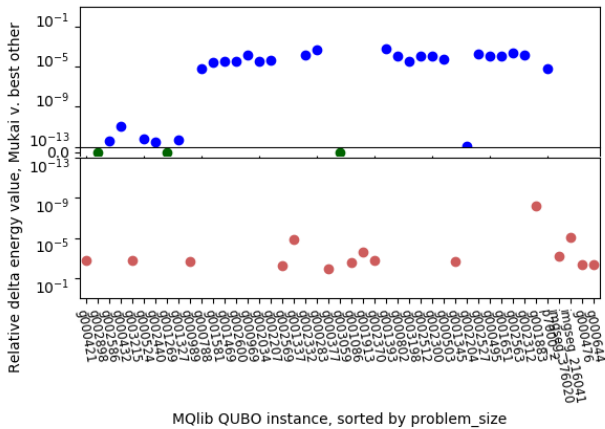
Fig. 1 concisely illustrates the energy results we obtained. For Fig. 1(a), for each MQLib instance, we determined whether the best MQLib heuristic or QCI qbsolv got the best energy value and then calculated the *relative delta energy*, defined as the difference between the two energy values divided by the best MQLib heuristic value. If QCI qbsolv obtained the best energy value, the relative delta energy appears in the upper half of the plot in **blue**; if the best MQLib heuristic won, the relative delta energy value appears in the bottom half of the plot in **red**. If the best MQLib heuristic and QCI qbsolv tied, the point appears on the x-axis in **green**.

We plot the relative energy differences on a log scale so that all the differences are visible. Some readers may question whether to display relative differences as small as 10^{-13} , but the real-world value of a QUBO-solution energy difference is hard to judge; e.g., improving the energy of a folded protein by a slight amount might enable it to work better in unforeseen ways. We document the energy differences and leave assignment of real-world value to subject-matter experts solving real-world problems.

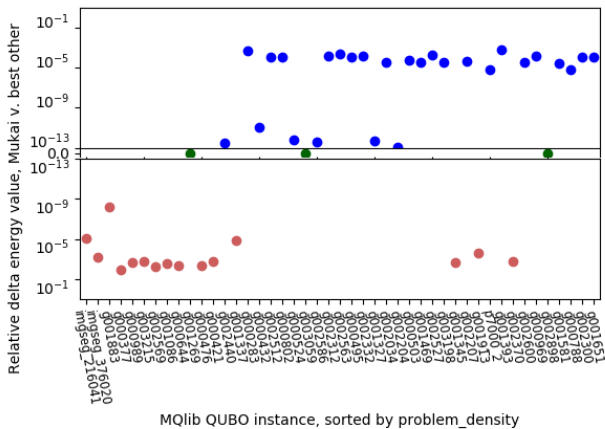
In Fig. 1(b), we sort the instances by increasing problem size, to see whether any patterns exist for which problems QCI qbsolv samples most effectively. Problem size, within the range of these problems, appears to have little effect



(a) Relative delta energy, sorted by increasing relative delta energy



(b) Relative delta energy, sorted by increasing problem size



(c) Relative delta energy, sorted by increasing problem density

Fig. 1: Relative delta energy, with instances sorted by 3 criteria

on QCI qbsolv’s energy performance relative to the MQLib heuristics. We note that we are targeting QCI qbsolv to effectively sample problems well above 50,000 variables, so the problem-size range exercised here is at the low end of our target.

Fig. 1(c) compares the MQLib heuristics and QCI qbsolv’s relative energy differences to problem density, and here a modest pattern does emerge, where the best MQLib heuristic is often better for sparser problems but QCI qbsolv is usually superior for denser problems. We have focused closely on the performance of solving sparse problems, so this is somewhat surprising and merits further investigation.

B. Time to Solution

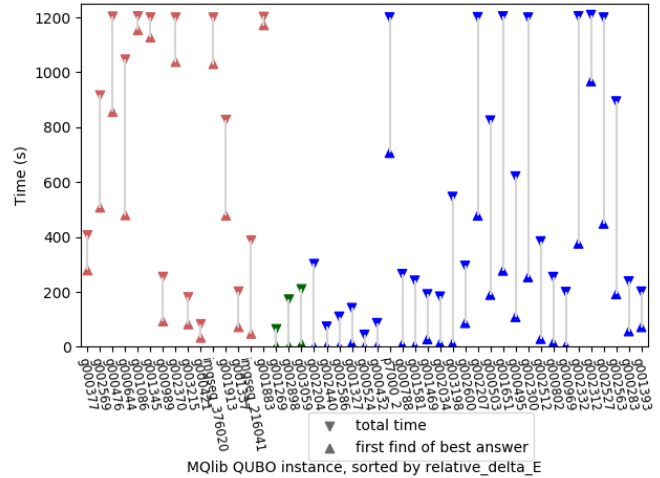
Fig. 2 illustrates, for the runs that produced the best energy values documented in Fig. 1, the time taken by QCI qbsolv. For each instance, two times are plotted, the first (Δ , at the bottom of the line) denoting the time when QCI qbsolv first found the best answer, and the second (∇ , at the top of the line) denoting the time when QCI qbsolv stopped searching for a better answer and ended. The instances are colored the same as Fig. 1(a) so that patterns of energy vis-a-vis time may be visually apparent. In Fig. 2(b,c) the problem size or problem density, respectively, is plotted for visual reference.

Fig. 2(a) sorts the instances by the same order as Fig. 1(a), i.e., increasing relative delta energy. Somewhat surprisingly, there appears to be little correlation between how the energy quality of the solutions QCI qbsolv finds and how long it requires to find those results. We see plenty of both red- and blue-capped lines that are relatively short. Not surprisingly, for the red-capped lines representing the problems on which QCI qbsolv did relatively poorly, it took more time, which matches what we want in a QUBO solver – in general, as long as there is a good prospect of better answers, keep trying. We interpret the several blue-capped lines in the right-most x-axis positions that hit the 1200s timeout as problems where QCI qbsolv is doing relatively well and yet believes it can do still better, so keeps trying.

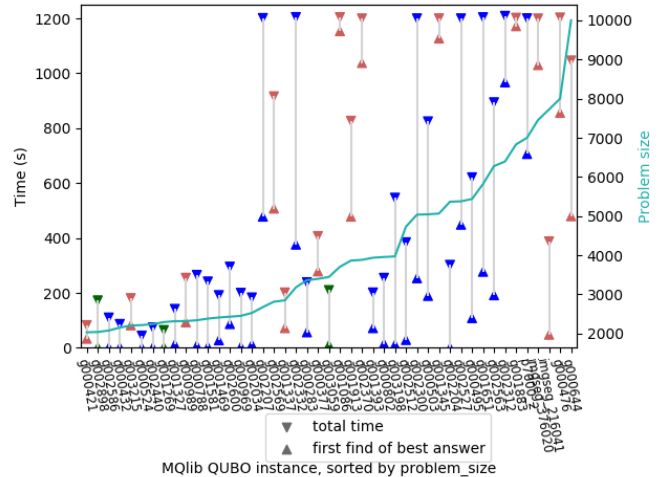
Turning to sampling time sorted by problem size, as shown in Fig. 2(b), we again see little pattern regarding on what instances QCI qbsolv performs best. Red- and blue-capped lines appear roughly randomly distributed through problem size.

In Fig. 2(c) we see sampling time sorted by problem density and detect a modest pattern again related to sparse problems, which when coupled with Fig. 1(c), indicates that QCI qbsolv is not sampling sparse problems particularly well and is taking more time than ideal to do so.

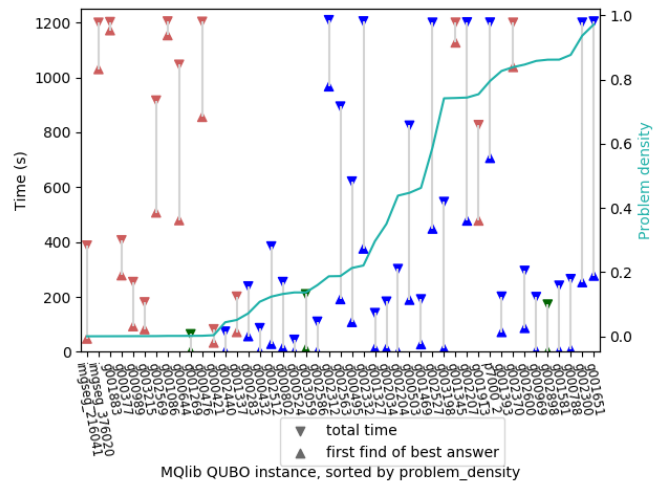
We deduce from the numerous long vertical lines, denoting QCI qbsolv executing for quite some time after having first found the best answer it found in that run, that there is room for improvement in QCI qbsolv’s heuristic for deciding that it is not making progress. (Note again that we configured QCI qbsolv for these runs to find the best



(a) Sampling time, sorted by increasing relative delta energy



(b) Sampling time, sorted by increasing problem size



(c) Sampling time, sorted by increasing problem density

Fig. 2: Sampling time, with instances sorted by 3 criteria

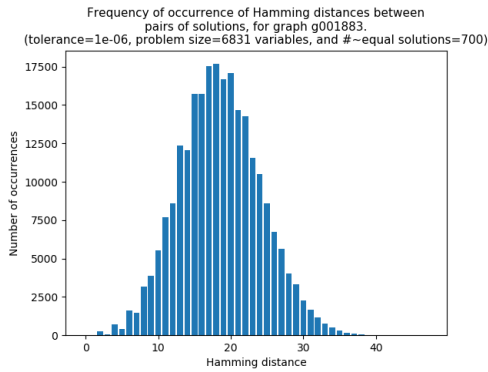


Fig. 3: Normal distribution of solution distances.

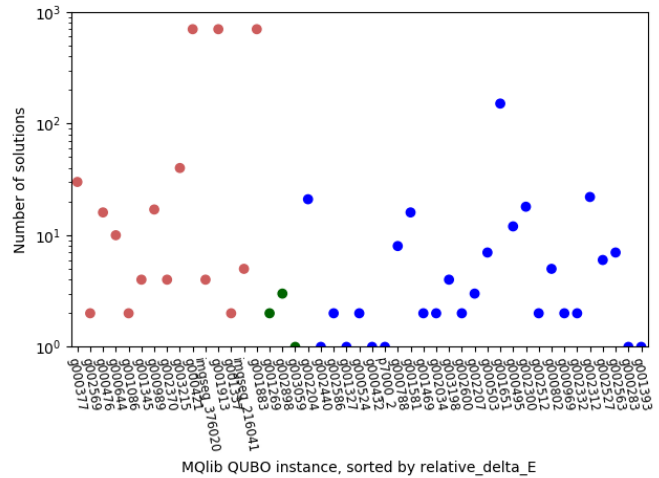
energy at some sacrifice of execution time, so we expect some degree of time overrun.)

C. Diversity

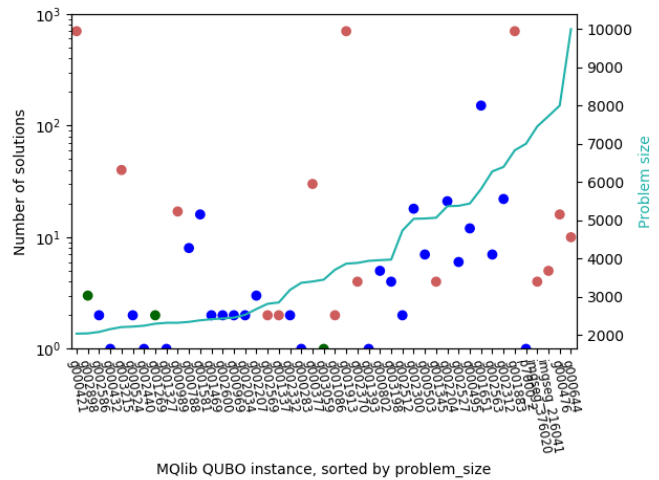
As noted above, diversity of *elite* solutions, i.e., those with energy equal (or nearly so) to the best solutions, is a valuable attribute of both a constrained-optimization sampler and a QC. We are not aware of accepted common metrics for representing diversity beyond the obvious use of Hamming distance to denote the difference between a pair of solutions. As noted above, all of our diversity calculations use a tolerance in the relative delta energy between a solution and the best solution found; for these calculations, that value was set to 10^{-6} .

A simple metric is the number of elite solutions, which we plot in Fig. 4 per instance, sorted respectively by relative delta energy, problem size, and problem density. We observe that the number of elite solutions shows no discernible correlation by any of those criteria, though unfortunately the most elite solutions (the maximum of 700) were found for 3 instances for which QCI qbsolv did not find the best known energy.

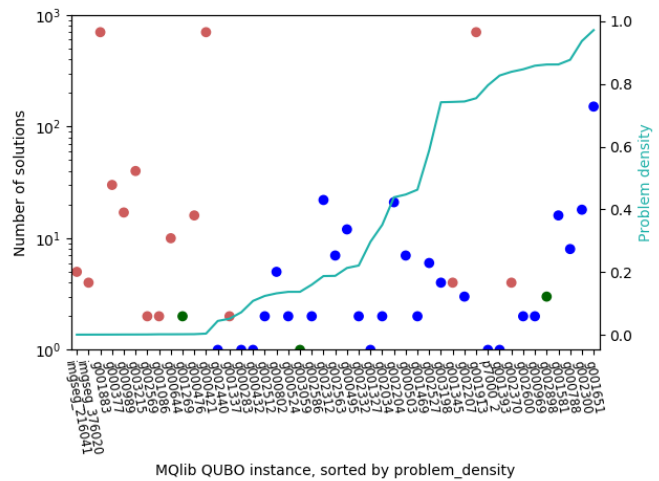
Further studying the similarity of solutions vectors, we consider the distribution and cluster properties of solutions. In Fig. 5-6, we selected three separate problems for which Mukai found the best known energy and considered the set of elite solutions within a relative tolerance of 10^{-6} . Each subfigure in Fig. 5-6 contains a matrix of distances between pairs of these elite solutions, a dendrogram on the top showing the hierarchical clustering of the elite solutions, a colorbar recording Hamming distance, both normalized and (nonnormalized), plus an inset histogram showing the distribution of distances. Each matrix is sorted according to the hierarchical clustering measured by its dendrogram (above the matrix), where the height of the lines in the dendrogram denotes the Hamming distance. The histogram is computed by counting the number of pairs of distinct solutions per Hamming distance. For instance, for a set of solutions uniformly distributed in a small region of space, the histogram would approximate a normal distribution, by the law of large numbers. Figure 3 shows this distribution



(a) Number of distinct elite solutions, sorted by increasing relative delta energy



(b) Number of distinct elite solutions, sorted by increasing problem size



(c) Number of distinct elite solutions, sorted by increasing problem density

Fig. 4: Diversity (number of distinct elite solutions), with instances sorted by 3 criteria

for a problem (g001883) with 700 near-equal solutions. A significant feature of many other problems is multiple solution regions in space and a relatively uniform distribution within each of these regions of space. Among the subplots in Fig. 5-6, the solutions differ from each other by Hamming distances (numbers of bit flips) ranging from one to hundreds. Of note, in terms of quality, they are equal to within a relative tolerance of 10^{-6} , giving the user a wide range of valid solutions. Just as a relatively minor change in energy may yield significantly improved results, for applications from airline scheduling to protein folding, it is often more important to have a pool of high-quality solutions, since out-of-problem factors such as business logic or production limitations may reduce the viability of a significant portion of those solutions.

D. Miscellany

The QCI qbsolv component of Mukai finds excellent energy values for many of the MQLib instances chosen by other groups of industrial benchmarks, and there is headroom for improvement in its performance, notably for sparser problems. We discovered that 9 of the selected MQLib instances appear not to meet the selection criteria of only a single heuristic achieving the best known solution, so those instances are not as hard as expected.¹ Due to the limited detail in [14], we cannot compare our results to those of their hybrid solver.

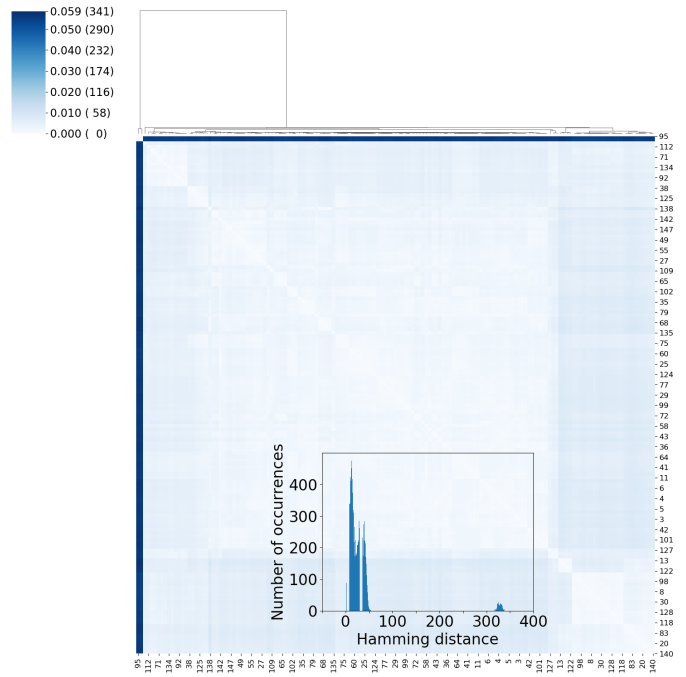
QCI qbsolv samples many MQLib instances very fast, in less than 25% of the 1200-second time limit established by MQLib. Still, there is room for faster time to solution by better recognition of lack of progress.

Diversity of solutions is perhaps an underappreciated dimension of solver performance on which QCI qbsolv performs very well, finding as many as 150 distinct superior solutions for one instance and finding distinct superior solutions with Hamming distances of 350 for others. Given QCs' exploitation of quantum effects to find widely separated solutions, having a classical solver that emulates that diversity today is an excellent means of being quantum-ready in an unexpected dimension.

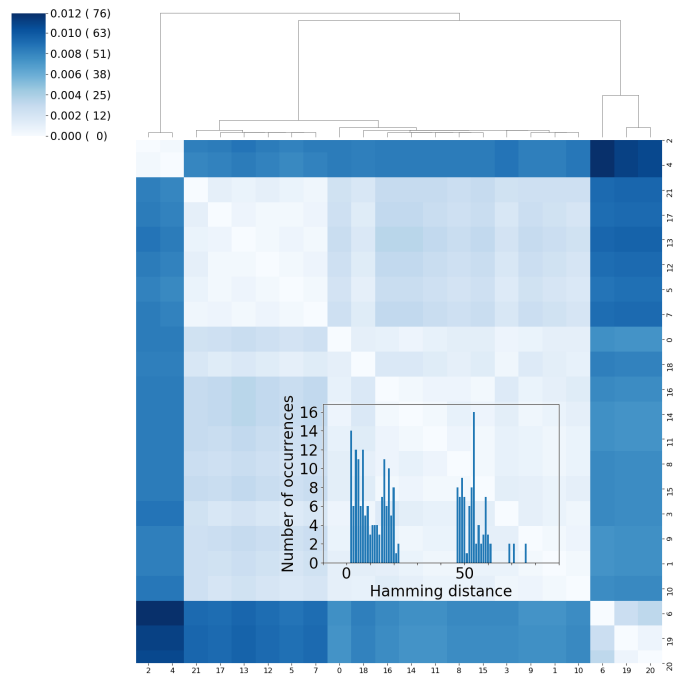
Having explored this set of 45 MQLib instances in detail, we see that expanding our scope to include larger MQLib problems will more accurately reflect the needs of industrial users needing to become quantum-ready.

As expected for an emerging technology like Mukai, there are numerous ways to improve these early results, including examining poorly performing instances for insight into improvements, using more classical compute resources (CPU cores or GPUs), moving to higher-level formulations that enable better performance and ease of use, and optimizing the benefit gained from near-term QCs via better hybrid quantum/classical methods. We have several developments under way to deploy much greater classical resources.

¹g000432, g000524, g001269, g001883, g002204, g002440, g002586, g002898, and g003215

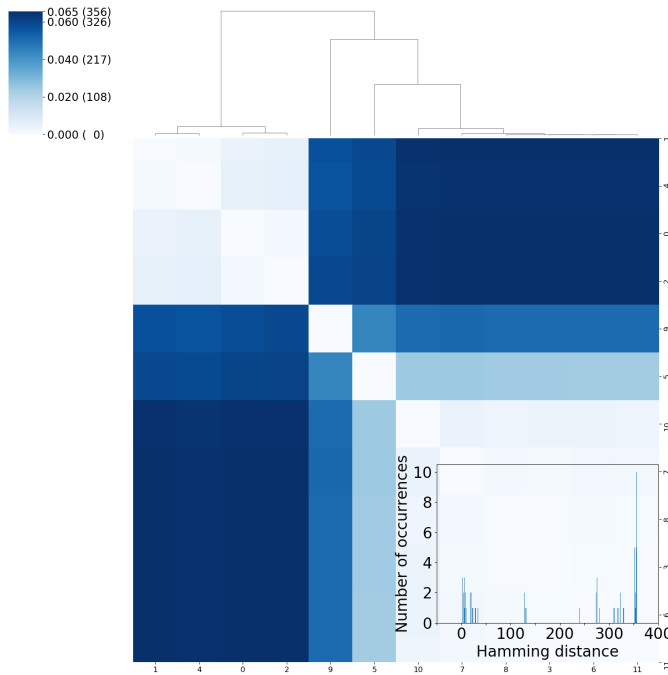


(a) Hamming distance information for g001651 solutions



(b) Hamming distance information for g002312 solutions

Fig. 5: Hamming distance information for solutions of two problem instances. (a) Most solutions are found very close together, with another cluster a Hamming distance of over 350 away. Within the large cluster the distribution is uniform and is aggregated into a single cluster early in the hierarchical clustering algorithm. This large cluster merges late with the small cluster. (b) The trimodal nature of the solutions is clear in the distance matrix and dendrogram, where the regions merge late in the dendrogram.



(a) Hamming distance information for g000495 solutions

Fig. 6: With the same context as Fig. 5, solutions were found in four places significantly far apart in space. Three of them were greater than a Hamming distance of 200 apart, with numerous solutions up to a distance of 350 apart.

We will soon release a higher-level API that will make it easier for application developers to specify constrained-optimization problems to Mukai and simultaneously grant to Mukai developers more design freedom to optimize problems before converting them to QUBO form. We are collaborating with an external partner on calibrating QAOA for effective use on near-term gate-model QCs.

This work reports on solving QUBOs from a well-known public benchmark repository. An important future step, translating this low-level benefit to an end-user benefit in solving real-world problems, will be vital to establishing the reality and value of this approach.

IV. CONCLUSIONS

We have shown that instances of the established QUBO formulation from multiple problem domains can be solved today on classical hardware with quantum-ready algorithms, delivering superior results in both quality of solution and diversity of solutions. The approach is also affordable, delivering, in many cases, superior performance on affordable hardware that is readily available in public cloud services. As expected for an emerging technology, there are numerous ways to improve these early results, including examining poorly performing instances, using more classical compute resources, moving to higher-level formulations that enable better performance and ease of use, and optimizing the benefit gained from near-term

QCs. Still, QCI's Mukai delivers the best known quality of results, time to solution, and diversity of solutions in a commercially available service, enabling compute-dependent organizations to become quantum-ready today.

ACKNOWLEDGMENT

We acknowledge the contributions that Max Dechantsreider of Performance Jones LLC made to the performance of QCI qbsolv.

REFERENCES

- [1] Michael Booth, Edward Dahl, Mark Furtney, and Steven P Reinhardt. Abstractions considered helpful: a tools architecture for quantum annealers. In *2016 IEEE High Performance Extreme Computing Conference (HPEC)*, pages 1–2. IEEE, 2016.
- [2] Gary Kochenberger, Jin-Kao Hao, Fred Glover, Mark Lewis, Zhipeng Lü, Haibo Wang, and Yang Wang. The unconstrained binary quadratic programming problem: a survey. *Journal of Combinatorial Optimization*, 28(1):58–81, 2014.
- [3] Sanjeeb Dash. A note on qubo instances defined on chimera graphs. *arXiv preprint arXiv:1306.1202*, 2013.
- [4] Andrew Lucas. Ising formulations of many NP problems. *Frontiers in Physics*, 2:5, 2014.
- [5] Phil Goddard, Susan Mniszewski, Florian Neukart, Scott Pakin, and Steve Reinhardt. How will early quantum computing benefit computational methods? In *Proc. SIAM Annual Meeting*, 2017.
- [6] Susan M Mniszewski, Christian Francisco Negre, and Hayato Montezuma Ushijima-Mwesigwa. Graph partitioning using the D-Wave for electronic structure problems. Technical report, Los Alamos National Lab.(LANL), Los Alamos, NM (United States), 2016.
- [7] Vikram Khipple Mulligan, Hans Melo, Haley Irene Merritt, Stewart Slocum, Brian D Weitzner, Andrew M Watkins, P Douglas Renfrew, Craig Pelissier, Paramjit S Arora, and Richard Bonneau. Designing peptides on a quantum computer. *bioRxiv*, page 752485, 2019.
- [8] Florian Neukart, Gabriele Compostella, Christian Seidel, David Von Dollen, Sheir Yarkoni, and Bob Parney. Traffic flow optimization using a quantum annealer. *Frontiers in ICT*, 4:29, 2017.
- [9] Hiroataka Irie, Goragot Wongpaisarnsin, Masayoshi Terabe, Akira Miki, and Shinichirou Taguchi. Quantum annealing of vehicle routing problem with time, state and capacity. In *International Workshop on Quantum Technology and Optimization Problems*, pages 145–156. Springer, 2019.
- [10] Gili Rosenberg, Mohammad Vazifeh, Brad Woods, and Eldad Haber. Building an iterative heuristic solver for a quantum annealer. *Computational Optimization and Applications*, 65(3):845–869, 2016.
- [11] Michael Booth, Steven P Reinhardt, and Aidan Roy. Partitioning optimization problems for hybrid classical/quantum execution. https://github.com/dwavesystems/qbsolv/blob/master/qbsolv_techReport.pdf, August 2017.
- [12] Edward Farhi, Jeffrey Goldstone, and Sam Gutmann. A quantum approximate optimization algorithm. *arXiv preprint arXiv:1411.4028*, 2014.
- [13] Iain Dunning, Swati Gupta, and John Silberholz. What works best when? a systematic evaluation of heuristics for Max-Cut and QUBO. *INFORMS Journal on Computing*, 30(3):608–624, 2018.
- [14] D-Wave Systems. D-Wave Hybrid Solver Service: An overview. https://www.dwavesys.com/sites/default/files/14-1039A-A_D-Wave_Hybrid_Solver_Service_An_Overview.pdf, March 2020.
- [15] Catherine C McGeoch. Principles and guidelines for quantum performance analysis. In *International Workshop on Quantum Technology and Optimization Problems*, pages 36–48. Springer, 2019.